Optical properties of silicon nanocrystals embedded in a SiO_2 matrix

L. Ding,[1] T. P. Chen,[1,*] Y. Liu,[1] C. Y. Ng,[1] and S. Fung[2]
[1]*School of Electrical and Electronic Engineering, Nanyang Technological University, 639798 Singapore*
[2]*Department of Physics, The University of Hong Kong, Hong Kong*
(Received 7 April 2005; revised manuscript received 22 July 2005; published 14 September 2005)

Optical properties of isolated silicon nanocrystals (*nc*-Si) with a mean size of ~4 nm embedded in a SiO_2 matrix that was synthesized with an ion beam technique have been determined with spectroscopic ellipsometry in the photon energy range of 1.1–5.0 eV. The optical properties of the *nc*-Si are found to be well described by both the Lorentz oscillator model and the Forouhi-Bloomer (FB) model. The *nc*-Si exhibits a significant reduction in the dielectric functions and optical constants and a large blueshift (~0.6 eV) in the absorption spectrum as compared with bulk crystalline silicon. The band gap of the *nc*-Si obtained from the FB model is ~1.7 eV, showing a large band gap expansion of ~0.6 eV relative to the bulk value. The band gap expansion is in very good agreement with the first-principles calculation of the *nc*-Si optical gap based on quantum confinement.

DOI: 10.1103/PhysRevB.72.125419 PACS number(s): 78.67.Bf

I. INTRODUCTION

Silicon nanocrystals (*nc*-Si) embedded in a SiO_2 matrix are extensively studied as they provide the possibilities for applications in Si-based optoelectronic devices, memory devices, and single electron devices with the advantage of being compatible with the mainstream complimentary metal-oxide-semiconductor (CMOS) process.[1–7] One of the promising techniques to form such a *nc*-Si structure is the implantation of silicon ions into a SiO_2 matrix followed by thermal annealing.[5–7] In this paper, we present a study on optical properties of the *nc*-Si embedded in a SiO_2 matrix synthesized with this technique. Such a study is obviously important to the fundamental physics as it is concerned with a system of quasiparticles with a size of less than ~5 nm isolated by a dielectric matrix, and it is also necessary to optoelectronic and photonic applications of the *nc*-Si.

Some theoretical calculations of optical properties of semiconductor nanocrystals have been reported. There are calculations of optical properties of *nc*-Si using various methods such as the empirical-pseudopotential approach and *ab initio* technique.[8–10] Recently, first-principles calculations of optical properties of Si and Ge nanocrystallites have been reported.[11–13] In contrast, few experimental studies of optical properties of *nc*-Si have been reported. Especially, it is difficult to experimentally determine the optical properties of *nc*-Si embedded in a dielectric matrix. Some experimental studies of the optical properties of a continued silicon nanocrystal thin film[14] and SiO_2/nanocrystalline Si multilayers[15] have been reported recently. In our preliminary studies, we have also reported the optical properties of *nc*-Si embedded in a SiO_2 matrix in the photon energy range of 1.1–3.1 eV.[16,17] Nevertheless, a comprehensive experimental study of the optical properties in a wider photon energy range and a proper modeling to the optical properties are still lacking. In this work, the optical properties including optical constants, absorption coefficient, and dielectric functions of the *nc*-Si embedded in a SiO_2 matrix in the photon energy range of 1.1–5.0 eV have been determined with spectroscopic ellipsometry (SE). The optical properties of *nc*-Si are modeled with the Lorentz oscillator model[18] and the Forouhi-Bloomer (FB) formulism.[19] The modeling based on the Lorentz oscillator model gives the information related to electron transitions, while the FB modeling yields the energy band gap of the *nc*-Si. A strong dielectric suppression and a large band-gap expansion are observed for the *nc*-Si.

II. EXPERIMENT

The *nc*-Si embedded in a SiO_2 matrix was synthesized by Si^+ implantation with a dose of 1×10^{17} atoms/cm^2 at an energy of 100 keV into a 550-nm-thick SiO_2 film thermally grown on a *p*-type Si substrate. A thermal annealing at 1000 °C for 30 min in nitrogen gas was carried out for the formation of Si nanocrystals. Figure 1 shows the high-resolution transmission electron microscopy (HRTEM) image of the *nc*-Si embedded in the SiO_2 matrix. The average

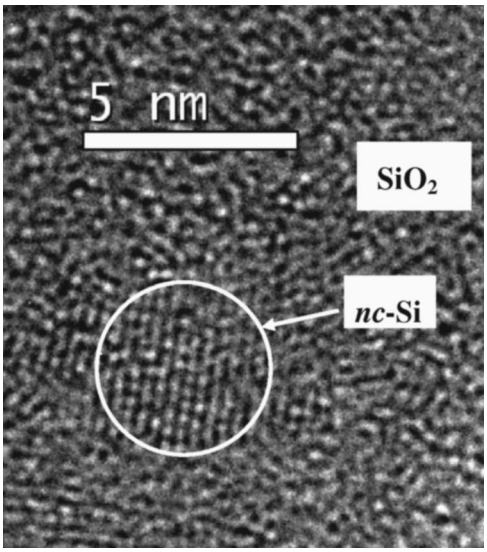

FIG. 1. HRTEM image of *nc*-Si embedded in SiO_2.

size of *nc*-Si determined from the broadening of the Bragg peak in the x-ray diffraction (XRD) spectrum is ~4.2 nm, which is consistent with the HRTEM measurement. The SE measurements were carried out in the wavelength range of 250–1100 nm with a step of 5 nm, and the incidence angle was set to 75°.

The *nc*-Si distribution in the SiO_2 thin film can be determined from the secondary ion mass spectroscopy (SIMS) measurement. The SIMS intensity $I(x)$ due to the excess silicon in the Si^+-implanted region at a given depth x can be obtained by deducting the Si SIMS signal of the pure SiO_2 region from the measured total Si SIMS signal (which is from both the excess Si and the SiO_2) at the depth. The amount of excess Si at depth x should be proportional to the intensity $I(x)$. The volume fraction of *nc*-Si at the depth should be proportional to the amount of the excess Si at the depth. Thus, the volume fraction $f(x)$ of the *nc*-Si embedded in SiO_2 at depth x can be expressed as

$$f(x) = \frac{QI(x)}{N_{Si}\int_0^{d_{\max}} I(x)dx}, \tag{1}$$

where Q is the dose of implanted Si ions in the unit of atoms/cm^2, d_{max} is the maximum depth in SiO_2 beyond which no excess Si can be detected, and N_{Si} is the Si density in the unit of atoms/cm^3. In this study, Q is equal to 1×10^{17} atoms/cm^2, and N_{Si} is 5×10^{22} atoms/cm^3.

III. MODELING AND DISCUSSIONS

The volume fraction of the *nc*-Si in the SiO_2 calculated from the SIMS measurement as a function of the depth is shown in Fig. 2. As can be seen in this figure, the *nc*-Si distributes from the surface of the SiO_2 film to a depth of 250 nm and there is almost no *nc*-Si in the SiO_2 film beyond a depth of 250 nm. Therefore, the thin film system can be divided into two layers, namely, the first layer ($0 \leqslant$ depth $\leqslant 250$ nm) with *nc*-Si distributing in SiO_2, and the second layer (depth >250 nm), which is just a basically pure SiO_2 layer without *nc*-Si. In the first layer, the optical properties vary with the depth as the volume fraction of the *nc*-Si varies with depth. In order to model the optical properties of the first layer, it is divided into m sublayers with equal thickness d_0 ($m=25$ and $d_0=10$ nm in this study). Each sublayer has a *nc*-Si volume fraction ($f_i, i=1,2,\ldots,m$) which can be calculated from the SIMS measurement, and the *nc*-Si volume fraction is considered to be constant within each sublayer. Each sublayer has its own effective dielectric function $\varepsilon_i (i=1,2,\ldots,m)$ due to its own *nc*-Si volume fraction. As such, the optical system in the SE analysis can be described with the multilayer model shown in Fig. 2. Each sublayer can be optically schematized as an effective medium, in which the SiO_2 is the host matrix while the *nc*-Si is an inclusion embedded in the SiO_2 matrix, represented by the Maxwell-Garnett effective medium approximation (EMA)

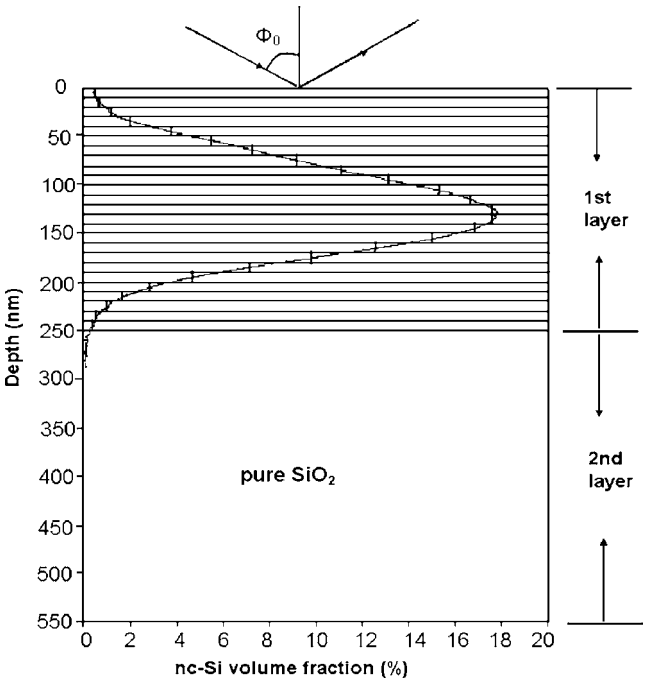

FIG. 2. Multilayer model used in the SE analysis. The *nc*-Si volume fraction is calculated from the SIMS measurement.

$$\frac{\varepsilon_i - \varepsilon_{SiO_2}}{\varepsilon_i + 2\varepsilon_{SiO_2}} = \frac{\varepsilon_{nc\text{-}Si} - \varepsilon_{SiO_2}}{\varepsilon_{nc\text{-}Si} + 2\varepsilon_{SiO_2}} f_i. \tag{2}$$

In Eq. (2), ε_i ($=N_i^2$, where N_i is the complex refractive index of the ith sublayer) is the effective complex dielectric function of the ith sublayer, ε_{SiO_2} is the dielectric function of SiO_2 matrix, $\varepsilon_{nc\text{-}Si}$ [$=(n_{nc\text{-}Si}-ik_{nc\text{-}Si})^2$, where $n_{nc\text{-}Si}$ and $k_{nc\text{-}Si}$ are the refractive index and extinction coefficient of the *nc*-Si, respectively] is the complex dielectric function of the *nc*-Si, and f_i is the volume fraction of *nc*-Si in the ith sublayer. As the volume fraction (f_i) and ε_{SiO_2} are known from Eq. (2), the effective complex dielectric function ε_i (and thus the effective complex refractive index N_i) for the ith sublayer ($i=1,2,\ldots,m$) can be expressed in terms of $\varepsilon_{nc\text{-}Si}$ (or the refractive index and extinction coefficient of *nc*-Si). Therefore, in the SE analysis, the ellipsometric angles (ψ and Δ) can be expressed as functions of the optical constants of the *nc*-Si, although these functions cannot be displayed with analytical formulas due to their complexity. Based on these functions, a spectral fitting to the experimental data of ψ and Δ can yield the dielectric function and optical constants of the *nc*-Si at various wavelengths. In the spectral fitting, an appropriate optical dispersion model should be used to describe the spectral dependence of dielectric function and the optical constants of the *nc*-Si. In the present work, two optical dispersion models, the Lorentz oscillator model[18] and the four-term Forouhi-Bloomer (FB) model,[19] were used to carry out the spectral fitting.

It is found that a combination of four Lorentz oscillators with different resonant energies is necessary to describe the spectral dependence of optical properties of the *nc*-Si embedded in SiO_2 over the wavelength range of 250 to 1100 nm.

TABLE I. Values of the parameters A_i, E_i, Γ_i ($i=1, 2, 3, 4$), and $\varepsilon_1(\infty)$ of the Lorentz oscillator model for both bulk crystalline silicon and the *nc*-Si embedded in SiO_2.

	A_i	E_i (eV)	Γ_i (eV^2)	ε_1 (∞)
Bulk crystalline silicon	10.1124	3.4423	0.1407	3.803
	45.9013	3.7005	0.4823	
	92.2078	4.3172	0.5289	
	11.5679	5.3233	0.3823	
Si nanocrystals embedded in SiO_2	30.8123	3.5560	0.4313	6.209
	13.7089	4.0151	0.3681	
	5.4209	4.0529	0.2242	
	10.3012	5.161 35	0.8173	

The Lorentz oscillator model can be expressed as[18]

$$\varepsilon(E) = \varepsilon_1(\infty) + \sum_{i=1}^{4} \frac{A_i}{E_i^2 - E^2 - i\Gamma_i E}, \tag{3}$$

where $\varepsilon(\infty)$ refers to the dielectric constant at very large photon energies, A_i is the amplitude of the ith oscillator with the unit of (eV)^2, Γ_i is the damping factor of the ith oscillator with the unit of eV, and E_i is the resonant energy with the unit of eV.

Besides the Lorentz oscillator model, the four-term FB model is found to be another choice to get a reasonable spectral fitting. It should be pointed out that the FB model can yield not only the information of optical constants and dielectric functions, but also the band gap of the isolated *nc*-Si embedded in the SiO_2 matrix. The information of the *nc*-Si band gap is very important because a band-gap expansion (if any) is direct evidence of the quantum confinement effect. Based on the four-term FB model,[19] the optical constants including the refractive index and extinction coefficient of the *nc*-Si are given by

$$k(E) = \left(\sum_{i=1}^{4} \frac{A_i}{E^2 - B_i E + C_i} \right) (E - E_g)^2, \tag{4}$$

$$n(E) = n(\infty) + \sum_{i=1}^{4} \frac{B_{0_i} E + C_{0_i}}{E^2 - B_i E + C_i}, \tag{5}$$

where

$$B_{0_i} = \frac{A_i}{Q_i} \left(-\frac{B_i^2}{2} + E_g B_i - {E_g}^2 + C_i \right), \tag{6}$$

$$C_{0_i} = \frac{A_i}{Q_i} \left((E_g^2 + C_i) \frac{B_i^2}{2} - 2E_g C_i \right), \tag{7}$$

$$Q_i = \frac{1}{2} (4C_i - B_i^2)^{\frac{1}{2}}, \tag{8}$$

where A_i, B_i, and C_i ($i=1$, 2, 3, and 4) are some parameters related to electron transition, $n(\infty)$ is the refractive index when photon energy $E \to \infty$, and E_g is the energy band gap of the *nc*-Si.

The spectral fitting is carried out by freely varying the parameters of the models to minimize the following mean-square error (MSE):

$$MSE = \frac{1}{2N - M} \sum_{i=1}^{N} \left[\left(\frac{\psi_i^{cal} - \psi_i^{\exp}}{\sigma \psi_i^{\exp}} \right)^2 + \left(\frac{\Delta_i^{cal} - \Delta_i^{\exp}}{\sigma \Delta_i^{\exp}} \right)^2 \right], \tag{9}$$

where N is the number of data points in the spectra, M is the number of variable parameters in the model, σ is the standard deviation on the experimental data points, ψ^{exp} and Δ^{exp} are the measured values of the ψ and Δ, while ψ^{cal} and Δ^{cal} are the corresponding calculated values.[18] For an efficient spectral fitting, the initial values of parameters of the two models are taken equal to that of bulk crystalline silicon listed in Tables I and II. An excellent spectral fitting based on the above approach in a wide wavelength range of 250 to 1100 nm has been obtained, as shown in Fig. 3, in which the best-fit spectra based on the FB model and Lorentz oscillator model are both included. As can be seen in this figure, all the complicated spectra features of both ψ and Δ are fitted excellently.

The fittings can yield reasonable values of all the parameters of the models. The best-fit parameters for the *nc*-Si based on the Lorentz oscillator model and four-term FB model are given in Tables I and II, respectively. For comparison, the corresponding values for bulk crystalline silicon are also shown in the tables. For the Lorentz oscillator model, similar to bulk crystalline silicon, the *nc*-Si also has four oscillators with some small shifts in the resonant energies relative to that of bulk crystalline silicon. On the other hand, the most important finding from the FB modeling is the large band-gap expansion of the *nc*-Si. The band gap of the *nc*-Si is 1.74 eV, which shows a band-gap expansion of $\sim$0.6 eV as compared to the band gap of bulk crystalline silicon. A discussion on the band-gap expansion will be given later.

Using the values of the parameters of the *nc*-Si shown in Tables I and II, the complex dielectric function and the optical constants of the *nc*-Si are calculated with Eq. (3) for the Lorentz oscillator model or Eqs. (4) and (5) for the FB model. The dielectric function and optical constants of the *n*c-Si are shown in Figs. 4 and 5, respectively, in which the

TABLE II. Values of the parameters A_i, B_i, and C_i ($i=1, 2, 3, 4$), $n(\infty)$, and E_g of the FB model for both bulk crystalline silicon and the *nc*-Si embedded in SiO_2.

	A_i	B_i (eV)	C_i (eV^2)	n (∞)	E_g (eV)
Bulk crystalline silicon	0.0036	6.8811	11.8486	2.3688	1.12
	0.014	7.401	13.7473		
	0.0683	8.634	18.7952		
	0.0496	10.2339	26.5029		
Si nanocrystals embedded in SiO_2	0.0538	7.1119	12.7176	2.8237	1.7369
	0.0056	8.0157	16.0797		
	0.0603	8.0300	18.7101		
	0.0003	10.3227	33.6447		

results calculated with the above two optical dispersion models are both included. The dielectric function and the optical constants of bulk crystalline silicon are also included in the two figures for comparison. As can be seen in Figs. 4 and 5, the overall spectral features of optical properties of *nc*-Si are similar to that of bulk crystalline silicon. However, the *nc*-Si shows a significant reduction in the optical constants and dielectric function as compared with bulk crystalline silicon. It has been well established that reduction of the static dielectric constant becomes significant as the size of the quantum confined physical systems, such as quantum dots and wires, approaches the nanometric range.[8,20–22] However, the origin of the reduction in the static dielectric constant with the size is still not fully understood. It is often attributed to the opening of the gap, which should lower the polarizability, but it is also shown that the reduction is due to the breaking of polarizable bonds at the surface and is not due to the opening of the band gap induced by the confinement.[23]

In addition to the above comparison of dielectric function between the bulk crystalline Si and the *nc*-Si, it is also interesting to have a comparison to other nanostructured Si ma-

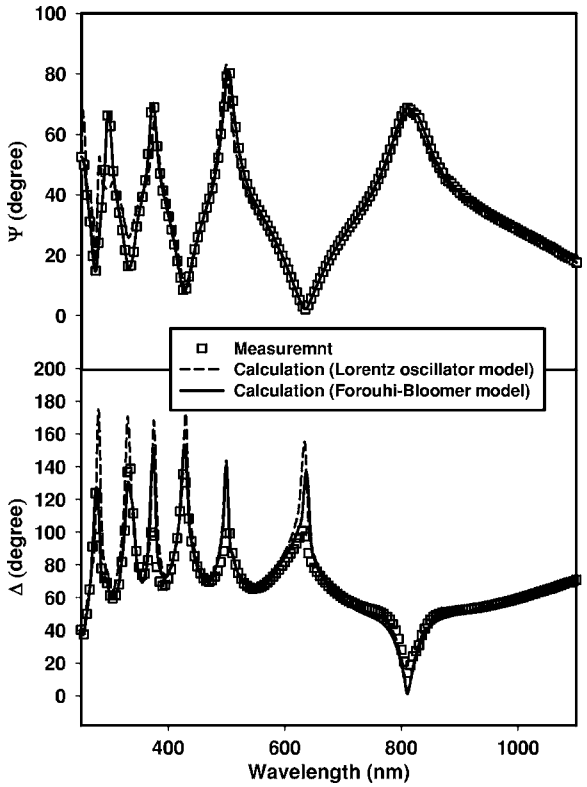

FIG. 3. Best spectral fittings of ψ and Δ based on the Lorentz oscillator model and the FB model with the approach described in the text.

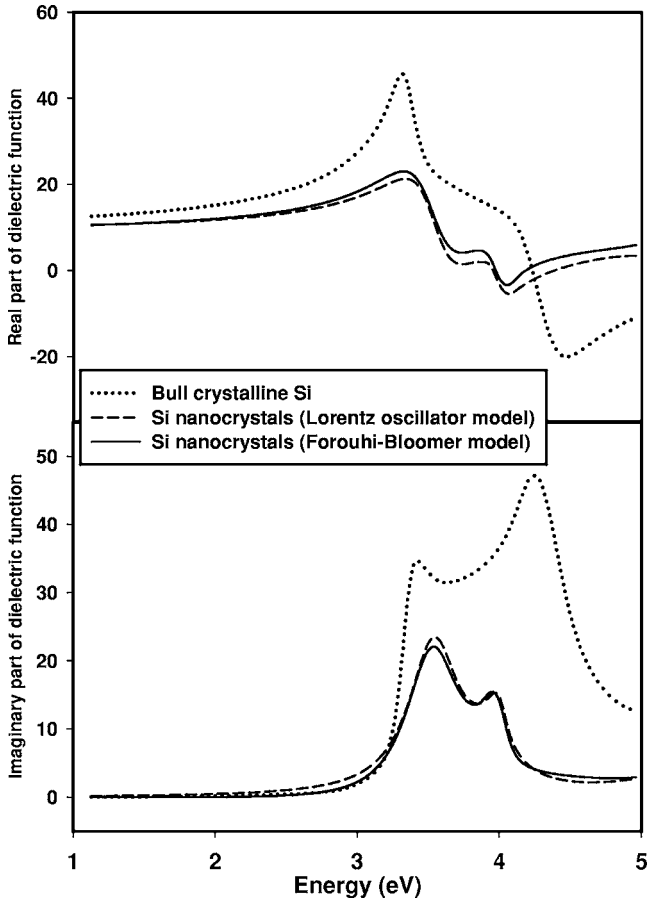

FIG. 4. Real (ε_1) and imaginary (ε_2) parts of the complex dielectric function of the *nc*-Si obtained from the spectral fittings based on the Lorentz oscillator model and the FB model. The dielectric function of bulk crystalline silicon is also included for comparison.

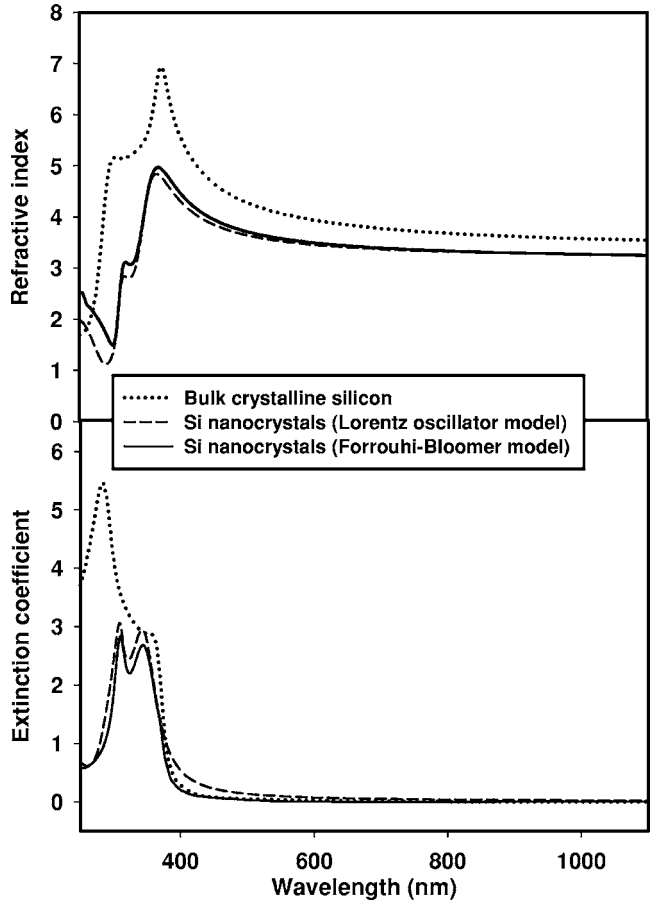

FIG. 5. Refractive index (n) and extinction coefficient (k) of the *nc*-Si and bulk crystalline silicon as functions of wavelength.

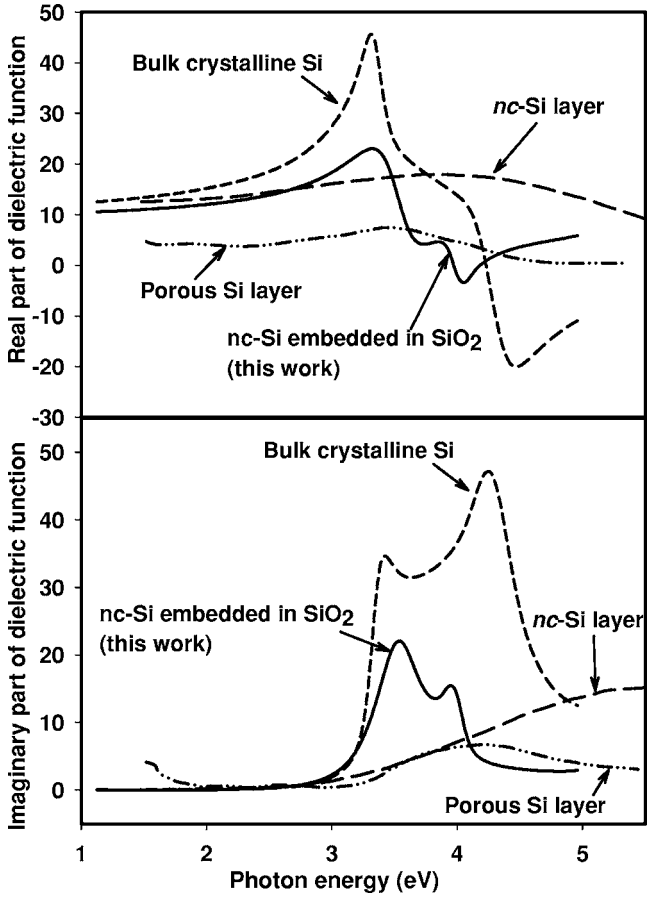

FIG. 6. Comparison of the dielectric function of *nc*-Si embedded in SiO_2 matrix based on the FB model to those of bulk crystalline Si, *nc*-Si layer [a hypothetical dense layer of *nc*-Si particles covered by their native oxide without voids (Ref. 14)] and porous Si layer of 70% porosity (Ref. 24).

terials. Figure 6 shows the comparison of dielectric function among the *nc*-Si embedded in SiO_2 matrix (this work), bulk crystalline Si, a porous Si layer with a porosity of 70%,[24] and a continuous *nc*-Si layer[14] (a hypothetical dense layer of *nc*-Si particles covered by their native oxide without voids). As pointed out previously, the spectral features of the *nc*-Si embedded in SiO_2 and bulk crystalline Si are similar. However, they are quite different from those of the porous Si layer and the *nc*-Si layer. This could be explained as below. For the porous Si layer, its dielectric function is affected by the pores and SiO_2 existing in the layer; for the *nc*-Si layer, although the porosity of the layer has been taken into account, the dielectric function is still affected by the native oxide of the nanocrystals.[14] In contrast, in the determination of the dielectric function of *nc*-Si embedded in the SiO_2 matrix, the effect of SiO_2 has been separated and there are no pores involved.

As mentioned previously, the *nc*-Si embedded in SiO_2 has a band-gap expansion of ~0.6 eV as compared to bulk crystalline silicon. The band-gap expansion is consistent with the blueshift of the plot of $(\alpha E)^{1/2}$ vs E (where α is the absorption coefficient and E is the photon energy), as shown in Fig. 7. The band gap of the *nc*-Si obtained by extrapolating the linear portion of the plot is 1.73 eV, which is almost the same as the value (1.74 eV) given in Table II. The band gap obtained in this work is in very good agreement with the first-principles calculation of the optical gap of silicon nanocrystals based on quantum confinement.[25] A fit to the calculation shown in Fig. 3 of Ref. 25 yields

$$E_g(D) = E_{g0} + C/D^n \tag{10}$$

where D is the nanocrystal size in nm, $E_g(D)$ is the band gap in eV of the nanocrystal, $E_{g0}=1.12$ eV is the band gap of bulk crystalline Si, $C=3.9$, and $n=1.22$. For the *nc*-Si size of 4.2 nm of this work, Eq. (10) gives a band gap of 1.79 eV, which is very close to the band-gap values mentioned above. The band gap of the *nc*-Si is also comparable to the energy of the photoluminescence (PL) peak. Figure 8 shows the room temperature PL spectrum of the *nc*-Si embedded in SiO_2. As shown in this figure, the PL intensity peaks at the photon energy of 1.61 eV, being similar to the result reported by Valenta[26] and the situation of 18% *nc*-Si in SiO_2 reported in Ref. 27. The band gap is larger than the PL peak energy by ~0.13 eV. This energy difference is about the same as the energy (0.134 eV) of the Si-O vibration peak (the Si-O stretching frequency is ~1083 cm^{-1}) of the system of *nc*-Si embedded in SiO_2 matrix.[28] This may suggest that the interface of *nc*-Si/SiO_2 plays an important role in the light emission.

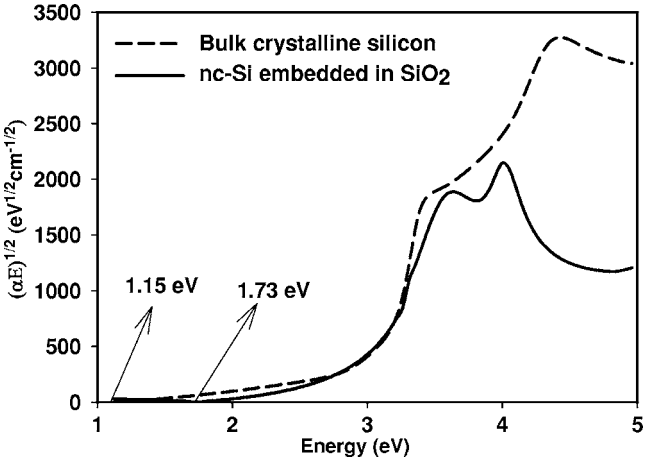

FIG. 7. Plot of $(\alpha E)^{1/2}$ versus photon energy (E) for *nc*-Si and bulk crystalline silicon. α denotes the absorption coefficient and is calculated with $\alpha=4\pi k/\lambda$, where k is the extinction coefficient and λ is the wavelength.

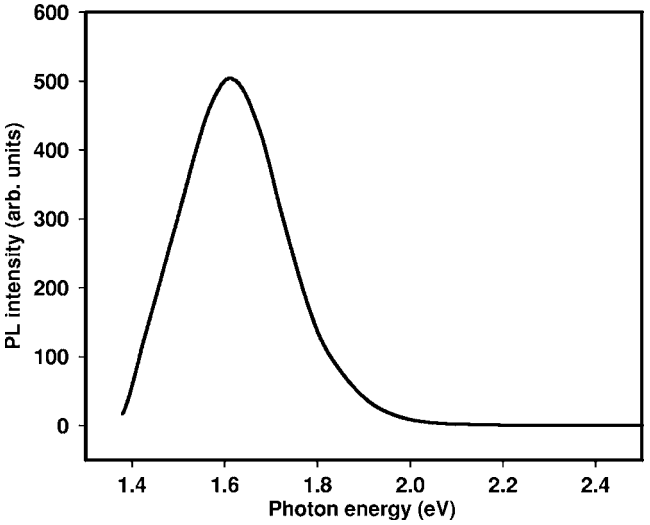

FIG. 8. Room temperature photoluminescence of *nc*-Si embedded in SiO_2 matrix. The wavelength of the excitation source is 355 nm.

IV. SUMMARY

In summary, we have developed an approach to determine the optical properties of *nc*-Si embedded in a SiO_2 matrix with spectroscopic ellipsometry based on the Maxwell-Garnett effective medium approximation as well as the SIMS measurements. Optical constants, absorption coefficient, and dielectric function of the *nc*-Si have been obtained in the photon energy range of 1.1–5.0 eV. The optical properties of the *nc*-Si are found to be well described by the four-term Forouhi-Bloomer model and the Lorentz oscillator model. The *nc*-Si shows a significant reduction in the optical constants and dielectric function as compared with bulk crystalline silicon. The band gap of the *nc*-Si is ~1.7 eV, showing a large band-gap expansion of ~0.6 eV. The band-gap expansion is in very good agreement with the first-principles calculation of the optical gap of silicon nanocrystals based on quantum confinement effect. The difference between the band gap and the PL peak is found to be about the same as the energy of the Si-O vibration peak, implying the role of the interface of *nc*-Si and/or SiO_2 in photoluminescence.

ACKNOWLEDGMENTS

This work has been financially supported by the Ministry of Education Singapore under Project No. ARC 1/04.

*Corresponding author. Electronic address: echentp@ntu.edu.sg

[1] R. A. Rao, R. F. Steimle, M. Sadd, C. T. Swift, B. Hradsky, S. Straub, T. Merchant, M. Stoker, S. G. H. Anderson, and M. Rossow, Solid-State Electron. **48**, 1463 (2004).
[2] D. N. Kouvatsos, V. Ioannou-Sougleridis, and A. G. Nassiopoulou, Appl. Phys. Lett. **82**, 397 (2003).
[3] S. H. Choi and R. G. Elliman, Appl. Phys. Lett. **75**, 968 (1999).
[4] S. Tiwari, F. Rana, H. Hanafi, A. Hartstein, E. F. Crabbé, and K. Chan, Appl. Phys. Lett. **68**, 1377 (1996).
[5] L. Pavesi, L. Dal Negro, C. Mazzoleni, G. Franzo, and F. Priolo, Nature (London) **408**, 440 (2000).
[6] N. Lalic, and J. Linnros, J. Lumin. **80**, 263 (1999).
[7] P. J. Walters, G. I. Bourianoff, and H. A. Atwater, Nat. Mater. **4**, 143 (2005).
[8] L.-W. Wang and Alex Zunger, Phys. Rev. Lett. **73**, 1039 (1994).
[9] C. Delerue, G. Allan, and M. Lannoo, Phys. Rev. B **48**, 11024 (1993).
[10] I. Vasiliev, S. Ogut, and J. R. Chelikowsky, Phys. Rev. Lett. **86**, 1813 (2001).
[11] H.-Ch. Weissker, J. Furthmüller, and F. Bechstedt, Phys. Rev. B **65**, 155327 (2002).
[12] H.-Ch. Weissker, J. Furthmüller, and F. Bechstedt, Phys. Rev. B **67**, 165322 (2003).
[13] H.-Ch. Weissker, J. Furthmüller, and F. Bechstedt, Phys. Rev. B **65**, 155328 (2002).
[14] D. Amans, S. Callard, A. Gagnaire, and J. Joseph, J. Appl. Phys. **93**, 4173 (2003).
[15] K.-J. Lee, T.-D. Kang, H. Lee, S. H. Hong, S.-H. Choi, T.-Y. Seong, K. J. Kim, and D. W. Moon, Thin Solid Films **476**, 196 (2005).
[16] T. P. Chen, Y. Liu, M. S. Tse, S. Fung, and Gui Dong, J. Appl. Phys. **95**, 8481 (2004).
[17] T. P. Chen, Y. Liu, M. S. Tse, O. K. Tan, P. F. Ho, K. Y. Liu, D. Gui, and A. L. K. Tan, Phys. Rev. B **68**, 153301 (2003).
[18] R. M. A. Azzam and N. M. Basharra, *Ellipsometry and Polarized Light* (North-Holland, Amsterdam, 1977).
[19] A. R. Forouhi and I. Bloomer, Phys. Rev. B **38**, 1865 (1988).
[20] D. R. Penn, Phys. Rev. **128**, 2093 (1962).
[21] R. Tsu, D. Babic, and L. Ioriatti, Jr., J. Appl. Phys. **82**, 1327 (1997).
[22] L.-W. Wang and Alex Zunger, Phys. Rev. B **53**, 9579 (1996).
[23] C. Delerue, M. Lannoo, and G. Allan, Phys. Rev. B **68**, 115411

(2003).
[24] U. Rossow, U. Frotscher, C. Pietryga, W. Richter, and D. E. Aspnes, Appl. Surf. Sci. **102**, 413 (1996).
[25] S. Ogut, J. R. Chelikowsky, and S. G. Louie, Phys. Rev. Lett. **79**, 1770 (1997).
[26] J. Valenta, J. Linnros, R. Juhasz, J.-L. Rehspringer, F. Huber, C. Hirlimann, S. Cheylan, and R. G. Elliman, J. Appl. Phys. **93**, 4471 (2003).
[27] M. Dovrat, Y. Goshen, J. Jedrzejewski, I. Balberg, and A. Sa'ar, Phys. Rev. B **69**, 155311 (2004).
[28] Y. Liu, T. P. Chen, Y. Q. Fu, M. S. Tse, P. F. Ho, J. H. Hsieh, Y. C. Liu, J. Phys. D **36**, L97 (2003).